CFD Letters 17, Issue 7 (2025) 1-17

CFD Letters

Journal homepage:
https://semarakilmu.com.my/journals/index.php/CFD_Letters/index
ISSN: 2180-1363

Modelling Time-Varying Subsurface Seepage in Unconfined Sloping Aquifers: A Comprehensive Analysis of Groundwater Flow with Nonlinear Advection-Diffusion Equations

Shikha Saxena[1], Chhaya Lande[2,*]

[1] RMD Sinhgad school of Engineering, Warje, Pune, India
[2] Symbiosis Institute of technology. Symbiosis International university, Lavale, Pune, India

ARTICLE INFO

Article history:
Received 5 October 2024
Received in revised form 6 November 2024
Accepted 9 December 2024
Available online 31 January 2025

Keywords:
Sloping aquifers; water table; Boussinesq equation; seepage; recharge

ABSTRACT

A stream-aquifer subsurface seepage model is developed to estimate fluctuations in the water table in an unconfined sloping aquifer which receives subsurface seepage from adjacent water bodies and time-varying vertical recharge. The groundwater flow is approximated by a nonlinear advection-diffusion equation subjected to time-dependent boundary conditions. Two numerical schemes namely Mac Cormack scheme and Du Fort Frankel scheme are used for solving the nonlinear flow equations. A Model is developed by solving the nonlinear Boussinesq equation using the Laplace transform technique. The combined effects of bed slope, stream rise rate, and vertical recharge are demonstrated using an illustrative example. To assess the validity of linearization, numerical solutions are compared with analytical solutions using an extensive value of aquifer parameters. Simulation is done using hypothetical data and results are compared with the previous literature. The results indicate that the approximate analytical solution agrees with the numerical solution for bed sloping angle within the range – 5 deg to 5 deg.

1. Introduction

Mathematical modeling plays a crucial role in understanding and managing groundwater resources [1]. Mathematical models allow researchers and water resource managers to predict how groundwater systems respond to various stresses and changes. Groundwater is a vital resource for drinking water, agriculture, industry, and ecosystems. Mathematical models help optimize the management of these resources by providing insights into sustainable extraction rates, recharge mechanisms, and contamination risks. In short, mathematical modelling is essential for comprehensively studying groundwater systems, optimizing resource management, assessing risks, designing engineering solutions, and facilitating informed decision-making in water resource management and environmental protection. The interaction between groundwater and surface water is a critical aspect of hydrology and water resource management. Groundwater and surface

* *Corresponding author.*
E-mail address: chhaya.lande@sitpune.edu.in (Chhaya Lande)

https://doi.org/10.37934/cfdl.17.7.117

water are interconnected components of the hydrological cycle. They often interact through processes such as infiltration, seepage, and discharge. Surface water can recharge groundwater aquifers through infiltration, while groundwater can discharge into surface water bodies such as springs wetlands, lakes and rivers. Hence the detailed study of these interaction processes is important for water managers to plan any water conservation policy. Surface-groundwater interaction modelling has been a crucial area of research for hydrogeologists and environmental engineers for many decades. These models serve not only to estimate surface-groundwater interactions but also to aid in comprehending various physical processes within integrated watershed systems. The flow of groundwater in the drenched zone is typically described by a partial differential equation, which is nonlinear. Finding a general solution to such differential equations is often not feasible. Consequently, analytical modelling yields only approximate closed-form solutions of the governing flow Eq. (1). Between the 1970s and 1980s, numerous models were developed to describe flow in permeable media. Many of these models relied on analytical as well as numerical solutions of the Boussinesq equation under various hydrological circumstances [2,3]. Shikha *et al.,* [4] developed an analytical model for groundwater variation and studied the effect of seepage and recharge. Some researchers addressed the nonlinearity of the flow equation using quasi-analytical approaches such as perturbation methods and the Adomian decomposition method [5,6]. However, even these methods require numerical validation of their analytical solutions. Several investigators have presented and tested essential numerical modeling techniques for validating analytical results. These techniques play a crucial role in ensuring the accuracy and reliability of the analytical solutions proposed. Overall, both analytical and numerical modeling approaches are essential tools for quantifying surface-groundwater interaction and understanding the complex dynamics of integrated watershed systems.

Numerical approaches have become integral in solving groundwater flow problems, especially with the advancement of high-speed computers. Several notable studies have employed numerical methods to address various aspects of groundwater flow dynamics: A study [7] utilized the perturbation method to develop a numerical solution for groundwater flow and investigated the combined bed leakage and its effect, partial infiltration through numerical simulation. Previous study [8] presented a numerical model. The numerical model mainly focuses on the stream/aquifer interactions and the transient variation in an alluvial valley aquifer. For horizontal unconfined aquifers, a one-dimensional flow which is generally represented Boussinesq equation is solved using a finite element method by a study [9]. Verhoest *et al.,* [10,11] and Pathania [12] introduced a numerically solved model and compared the results against a transient approximate analytical solution. Koussis and Lian [13], Teloglou and Zissis [14,15] conducted numerical investigations of streamflow toward waterways in soil deposits, considering constant or time-varying recharge. Rai and Manglik [16] explored fluctuations of the water table under the effect of constant time-varying recharge using analytical and numerical models. Jiang and Sun *et al.,* [17,18] introduced a new analytical solution to describe groundwater table fluctuation in a semi-infinite unconfined aquifer. The linearization technique is used to solve the Boussinesq equation. Validated against numerical solutions of the nonlinear Boussinesq equation. Antangana and Botha [19] employed the homotopic decomposition method to solve groundwater flow equations. Bansal *et al.,* [20-22] used a fully explicit predictor-corrector method to assess the efficiency of linearization of the Boussinesq equation. Lockington [23] studied the response of unconfined aquifers under the effect of various parameters. The sudden drawdown effect in the horizontal aquifer is presented by Parlange *et al.,* [24]. Hunt *et al.,* [25] presented the water table depletion due to pumping. Lande *et al.,* and Huang *et al.,* [26,27] studied the fluctuation of the water table under the effect of recharge and withdrawal. Shaikh and Hsieh *et al.,* [28,29] analysed the dynamic behaviour of tide-induced water table variations in an unconfined aquifer system, solving the nonlinear Boussinesq equation analytically and numerically. These studies demonstrate the versatility and effectiveness of numerical methods in addressing complex groundwater flow phenomena and validating analytical solutions, contributing significantly to the understanding of groundwater dynamics in various hydrogeological settings. They studied the impact of various parameters on groundwater mounding or a stream. A lagging theory is been introduced into the mathematical model of pump-induced confined flow where the aquifer is wedge-shaped by Ali *et al.,* [30]. The extensive review of the groundwater-surface water interaction phenomenon is being elaborated by Dolon and Lande *et al.,* [31,32]. Various water table fluctuation methods are explained by Becke [33] in their study. A flow pattern in heterogeneous medium is studied by Jaiswal *et al.,* [34].

Many researchers developed a mathematical model under various geological conditions by considering horizontal aquifer bases. The main limitations of the model presented in the literature are they do not address the combined effect of bed slope, recharge, and gradual variation of stream stage. Moreover, there are very few models developed using analytical methods.

In this paper, the water table fluctuation under the effect of bed slope, artificial recharge, and Variation in the adjacent water bodies is studied. The flow is represented by a nonlinear partial differential equation, characterizing the transient flow of subsurface seepage known as the Boussinesq equation, solved using two different numerical methods. The first one is a predictor-corrector scheme and the second one is based on the finite difference method. Numerical solutions are then compared with the analytical solution of the linearized Boussinesq equation to assess the validity of linearization. Two mathematical parameters namely the L2 norm and Tchebycheff norm are used to quantify variations in the analytical and numerical solutions.

2. Development of Analytical Model and its Numerical Solution

Figure 1 shows the model consists an unconfined aquifer which is resting on a downward sloping bed. A bed is impervious in nature. The aquifer is in contact with a stream of constant water head on the one end, while on the other end, a stream of the varying stage is considered. A constant downward recharge at a time varying rate is considered and effect of the recharge and stream variation is studied.

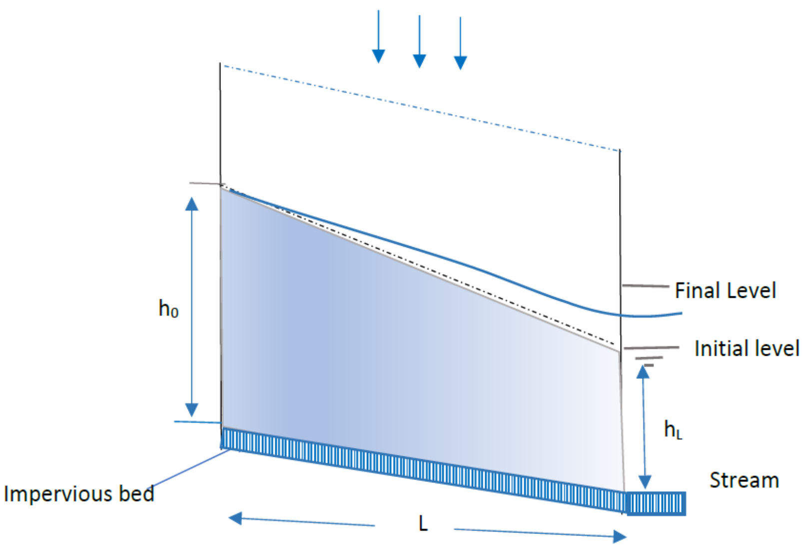

Fig. 1. A schematic diagram of an impervious aquifer laying on a sloping bed

The flow of subsurface seepage in the unconfined aquifer is governed by the following nonlinear partial differential equation;

$$K \cos^2\beta \frac{\partial}{\partial x}\left(\hbar\frac{\partial\hbar}{\partial x}\right) - K\sin\beta\cos\beta\frac{\partial\hbar}{\partial x} + \bar{N}(t) = S\frac{\partial\hbar}{\partial t}, \tag{1}$$

here

$\hbar$ denotes the water table height
K-hydraulic conductivity
S-specific yield
x-spatial coordinate
$\bar{N}(t)$-Time dependent recharge function

The recharge function is approximated in terms of exponential function as

$$\bar{N}(t) = N_0 + N_1 e^{-\lambda t}. \tag{2}$$

A positive constant λ used in this expression is characterizing the rate of recharge which decreases from an initial value $N_0 + N_1$ to a final value N_0.

A positive constant λ is the rate of recharge which varies from 0 to ∞ and gives the values from

$N_0 + N_1$ to N_0.

The initial conditions of the water table can be specified as

$$\hbar(x, t=0) = \hbar_0 - (\hbar_0 - \hbar_L)\frac{x}{L} \tag{3}$$

$\hbar_0$ is the water level at the left boundary of the aquifer. The right end of the aquifer is adjacent with stream whose water level is varying with respective to time. The stream levels are escalating from an initial level $\hbar_L$ to its final level $\hbar_0$ by an exponential function of time.
These conditions can be concise as

$$\hbar(x=0, t) = \hbar_0 \tag{4a}$$

$$\hbar(x=L, t) = \hbar_0 + (\hbar_L - \hbar_0)\ e^{-\gamma t} \tag{4b}$$

The parameter $-\gamma$ is the rise rate.

2.1 Mac Cormack Scheme

Mac Cormack scheme used by previous studies [5, 30], is widely used numerical second ordered finite difference scheme consisting of an explicit predictor and a corrector in which predictor is based on forward difference scheme, while corrector is based on backward difference scheme. Rewrite Eq. (1) as

$$K\cos^2\beta\frac{\partial}{\partial x}\left(\hbar\frac{\partial\hbar}{\partial x}\right)-\frac{K}{2}\sin 2\beta\frac{\partial\hbar}{\partial x}+N_0+N_1e^{-\lambda t}=S\frac{\partial\hbar}{\partial t} \tag{5}$$

$$A_1\frac{\partial}{\partial x}\left(\hbar\frac{\partial\hbar}{\partial x}\right)-A_2\frac{\partial\hbar}{\partial x}+\frac{N_0+N_1e^{-\lambda t}}{S}=\frac{\partial\hbar}{\partial t} \tag{6}$$

Where $A_1=\frac{K\,Cos2\beta}{S}$ *and* $A_2=\frac{K\,Sin2\beta}{2S}$. Eq. (6) can now be written as

$$A_1\left(h\frac{\partial^2\hbar}{\partial x^2}+\left(\frac{\partial\hbar}{\partial x}\right)^2\right)-A_2\left(\frac{\partial\hbar}{\partial x}\right)+\left(\frac{N_0+N(t)e^{-\lambda t}}{S}\right)=\frac{\partial\hbar}{\partial t} \tag{7}$$

In predictor step, the value of $\hbar$ is obtained by replacing the spatial and temporal values by forward difference, so Eq. (13) is rewritten as

$$\frac{\hbar_{k,n+1}-\hbar_{k,n}}{\Delta t}=A_1\left\{\frac{\hbar_{k,n}\left(\hbar_{k+1,n}-2\hbar_{k,n}+\hbar_{k-1,n}\right)+\left(\hbar_{k+1,n}-\hbar_{k,n}\right)^2}{(\Delta x)^2}\right\}-A_2\left(\frac{\hbar_{k+1,n}-\hbar_{k,n}}{\Delta x}\right)+\left(\frac{N_0+N_1e^{-\lambda n}}{S}\right) \tag{8}$$

Where Δx and Δt are mesh sizes along the x and t axis. Denoting $\hbar_{k,n+1}$ by $\hbar^*_{k,n+1}$ as the predicted value of the water head, Eq. (8) can be simplified as

$$\begin{aligned}\hbar^*_{k,n+1}=\hbar_{k,n}+\;&A_1\frac{\Delta t}{(\Delta x)^2}\left(\hbar_{k+1,n}\hbar_{k+1,n}-\hbar_{k+1,n}\hbar_{k,n}-\hbar_{k,n}\hbar_{k,n}+\hbar_{k,n}\hbar_{k-1,n}\right)-A_2\frac{\Delta t}{\Delta x}\left(\hbar_{k+1,n}-\hbar_{k,n}\right)\\&+\left(\frac{N_0+N_1e^{-\lambda n}}{S}\right)\Delta t\end{aligned} \tag{9}$$

The corrector method is obtained by replacing the space derivative by backward differences and the time derivative by forward difference. Simplifying the mathematical expressions and denoting the corrected value by $\hbar^{**}_{k,n+1}$ one obtains

$$\begin{aligned}\hbar^{**}_{k,n+1}=\;&\hbar_{k,n}+A_1\frac{\Delta t}{(\Delta x)^2}\left(\hbar^*_{k,n+1}\hbar^*_{k+1,n+1}-\hbar^*_{k,n+1}\hbar^*_{k,n+1}-\hbar^*_{k-1,n+1}\hbar^*_{k,n+1}+\hbar^*_{k-1,n+1}\hbar^*_{k-1,n+1}\hbar^*_{k-1,n}\right)\\&-A_2\frac{\Delta t}{\Delta x}\left(\hbar^*_{k,n+1}-\hbar^*_{k-1,n+1}\right)+\left(\frac{N_0+N_1e^{-\lambda n}}{S}\right)\Delta t\end{aligned} \tag{10}$$

The final value of $h_{k,n+1}$ is given as arithmetic mean of predictor and corrector step, i.e.

$$\hbar_{k,n+1} = \frac{1}{2}\left\{\begin{array}{l} \hbar_{k,n} + \hbar^{*}_{k,n+1} + A_1 \dfrac{\Delta t}{(\Delta x)^2}\left(\hbar^{*}_{k,n+1}\hbar^{*}_{k+1,n+1} - \hbar^{*}_{k,n+1}\hbar^{*}_{k,n+1} - \hbar^{*}_{k-1,n+1}\hbar^{*}_{k,n+1} + \hbar^{*}_{k-1,n+1}\hbar^{*}_{k-1,n+1}\right) \\ -A_2 \dfrac{\Delta t}{\Delta x}\left(\hbar_{k+1,n}\hbar_{k+1,n} - \hbar_{k+1,n}\hbar_{k,n} - \hbar_{k,n}\hbar_{k,n} + \hbar_{k,n}\hbar_{k-1,n}\right) \end{array}\right\} + \left(\frac{N_0 + N_1 e^{-\lambda n}}{2S}\right)\Delta t \tag{11}$$

The initial & boundary conditions are discretized as

$$\hbar_{k,1} = \hbar_0 - \left(\hbar_0 - \hbar_L\right)\frac{k\,\Delta x}{L} \tag{12a}$$

$$\hbar_{1,n+1} = \hbar_0 \tag{12b}$$

$$\hbar_{M,n+1} = \hbar_0 + \left(\hbar_L - \hbar_0\right)\; e^{-\gamma(n+1)\Delta t} \tag{12c}$$

Where M is the number of meshes along the $x-axis$. Mac Cormack is second order conditionally stable scheme. Numerical experiments reveal that the scheme is stable if

$$C_1 \frac{\Delta t}{(\Delta x)^2} \leq 0.01 \tag{13a}$$

$$C_2 \frac{\Delta t}{\Delta x} \leq 0.5 \tag{13b}$$

2.2 Du Fort Frankel Scheme

Eq. (1) is solved using a second numerical method which is second order, explicit Du Fort Frankel (DFF) scheme. The method is based on the Finite Difference Method and is absolutely convergent. The method is often used for the numerical solution of a parabolic partial differential equation. In two steps, one can Implement the scheme, namely $j \geq 2$ and $j = 1$, and n indicates mesh number along the time axis.

So, rewriting Eq. (1) as

$$\left\{h\frac{\partial^2\hbar}{\partial x^2} + \left(\frac{\partial\hbar}{\partial x}\right)^2\right\} - \tan\beta\,\frac{\partial\hbar}{\partial x} + \frac{N_0 + N_1\,e^{-\lambda t}}{K\cos^2\beta} = A_1\frac{\partial\hbar}{\partial t} \tag{14}$$

Where $A_1 = \dfrac{K\,Cos2\beta}{S}$.

Applying the central difference scheme and discretizing the time and spatial derivative of Eq. (14), gives

$$A_1\left(\frac{\hbar_{i,j+1}-\hbar_{i,j-1}}{2\Delta t}\right)=\left\{\frac{\hbar_{i,j}\left(\hbar_{i+1,j}-2\hbar_{i,j}+\hbar_{i-1,j}\right)}{\left(\Delta x\right)^2}+\frac{\left(\hbar_{i+1,j}-\hbar_{i-1,j}\right)^2}{\left(2\Delta x\right)^2}\right\}-\tan\beta\left(\frac{\hbar_{i+1,j}-\hbar_{i-1,j}}{2\Delta x}\right)+\left(\frac{N_0+N_1e^{-\lambda(j+1)\Delta t}}{K\cos^2\beta}\right) \tag{15}$$

Where $\hbar_{i,j+1}$ is the water head height at the current time step. Δx and Δt are respectively denote the mesh size along the x and t-axis. Using $\hbar_{i,j}=\frac{\hbar_{i,j-1}+\hbar_{i,j+1}}{2}$ in the Eq. (15) and simplifying it, one gets

$$\hbar_{i,j+1}\left(\frac{1}{2\Delta t}+\frac{\hbar_{i,j}}{A_1\left(\Delta x\right)^2}\right)=\frac{\hbar_{i,j-1}}{2\Delta t}+\frac{2\Delta t}{A_1}\left[\left(\frac{\hbar_{i+1,j}-\hbar_{i-1,j}}{2\Delta x}\right)^2-\tan\beta\left(\frac{\hbar_{i+1,j}-\hbar_{i-1,j}}{2\Delta x}\right)+\frac{\hbar_{i,j}\left(\hbar_{i+1,j}-\hbar_{i,j-1}+\hbar_{i-1,j}\right)}{\left(\Delta x\right)^2}\right]+\left(N_0+N_1e^{-\lambda(j+1)\Delta t}\right)\frac{\Delta t}{S} \tag{16}$$

Which leads to

$$\hbar_{i,j+1}=\frac{1}{\left(\frac{1}{2\Delta t}+\frac{\hbar_{i,j}}{A_1\left(\Delta x\right)^2}\right)}\left[\frac{\hbar_{i,j-1}}{2\Delta t}+\frac{2\Delta t}{A_1}\left\{\left(\frac{\hbar_{i+1,j}-\hbar_{i-1,j}}{2\Delta x}\right)^2-\tan\beta\left(\frac{\hbar_{i+1,j}-\hbar_{i-1,j}}{2\Delta x}\right)+\frac{\hbar_{i,j}\left(\hbar_{i+1,j}-\hbar_{i,j-1}+\hbar_{i-1,j}\right)}{\left(\Delta x\right)^2}\right\}+\left(N_0+N_1e^{-\lambda(j+1)\Delta t}\right)\frac{\Delta t}{S}\right] \tag{17}$$

Eq. (17) is the equation of water head height $\hbar_{i,j+1}$ for $j\geq 2$. In order to get the value of $\hbar_{i,j+1}$ at $j=1$.

According to normal techniques of discretization, a forward difference is applied to the temporal variables to discretize the central difference to space variables in the equation. The resulting equation becomes

$$A_1\left(\frac{\hbar_{i,j+1}-\hbar_{i,j}}{\Delta t}\right)=\left\{\frac{\hbar_{i,j}\left(\hbar_{i+1,j}-2\hbar_{i,j}+\hbar_{i-1,j}\right)}{\left(\Delta x\right)^2}+\frac{\left(\hbar_{i+1,j}-\hbar_{i-1,j}\right)^2}{\left(2\Delta x\right)^2}\right\}-\tan\beta\left(\frac{\hbar_{i+1,j}-\hbar_{i-1,j}}{2\Delta x}\right)+\left(\frac{N_0+N_1e^{-\lambda(j+1)\Delta t}}{K\cos^2\beta}\right) \tag{18}$$

Setting $j=1$ in the above equation, one gets

$$\hbar_{i,2} = \hbar_{i,1} + \frac{\Delta t}{A_1}\left\{\begin{array}{l}\dfrac{\hbar_{i,1}\left(\hbar_{i+1,1} - 2\hbar_{i,1} + \hbar_{i-1,1}\right)}{(\Delta x)^2} \\ + \dfrac{\left(\hbar_{i+1,1} - \hbar_{i-1,1}\right)^2}{(2\Delta x)^2}\end{array}\right\} - \tan\beta\left(\frac{\hbar_{i+1,1} - \hbar_{i-1,1}}{2\Delta x}\right) + \left(\frac{N_0 + N_1 e^{-2\lambda\Delta t}}{S}\right)\Delta t \tag{19}$$

The discretization of boundary conditions is given as

$$\hbar_{i,1} = \hbar_0 - \left(\hbar_0 - \hbar_L\right)\frac{i\,\Delta x}{L} \tag{20a}$$

$$\hbar_{1,j+1} = \hbar_0 \tag{20b}$$

$$\hbar_{i,j+1} = \hbar_0 + \left(\hbar_L - \hbar_0\right)\ e^{-\gamma(j+1)\Delta t} \tag{20c}$$

In the DFF scheme applied here the truncation error at the current instance is given by a parabolic equation

$$O(\Delta x_2) + O(\Delta t_2) + O\left\{\left(\frac{\Delta t}{\Delta x}\right)2\right\}$$

For the convergence of the scheme choose $\Delta t = 0.001\ \Delta x = 0.1$

3. Approximate Analytical Solution of Boussinesq Equation

In this section, an approximate analytical solution of the governing flow equation is presented which can be used as a validation tool for the numerical solutions. In order to order to obtain the approximate analytical solution, Eq. (1) is linearized using the technique of Marino [5]. The resulting equation is expressed as follows:

$$\frac{\partial^2 \hbar}{\partial x^2} - \frac{\tan\beta}{h}\frac{\partial \hbar}{\partial x} + \frac{N(t)}{K\hbar\cos^2\beta} = \frac{S}{K\hbar\cos^2\beta}\frac{\partial \hbar}{\partial t} \tag{21}$$

Where $\hbar$ is the average saturated depth of the aquifer (Marino [5]). Now define the following dimensionless variables which helps to understand the relation between variables using the techniques used by [35],

$$\bar{H} = \frac{\hbar - \hbar_0}{\hbar_L - \hbar_0}\ \ ;\ \tau = \frac{\left(K\hbar\cos^2\beta\right)t}{S\,L^2}\ ;\ \ X = \frac{x}{L}\ \ ;\ \alpha = \frac{L\tan\beta}{2\hbar} \tag{22}$$

Using these variables in Eq. (21) and simplifying, one gets

$$\frac{\partial^2 \bar{H}}{\partial X^2} - 2\alpha \frac{\partial \bar{H}}{\partial X} + \left(N_0{}' + N_1{}' e^{-\lambda_1 \tau} \right) = \frac{\partial \bar{H}}{\partial \tau} \tag{23}$$

Where,

$$N_0{}' = \frac{L^2 N_0}{Kh(\hbar_L - \hbar_0)\cos^2 \beta} \ ; \ \lambda_1 = \frac{\left(SL^2\right)\lambda}{Kh\cos^2 \beta} \ ; \ N_1{}' = \frac{L^2 N_1}{Kh(\hbar_L - \hbar_0)\cos^2 \beta} \tag{24}$$

The reduced initial and boundary conditions are as follows

$$\bar{H}(X, \tau = 0) = X \tag{25a}$$

$$\bar{H}(X = 0, \tau) = 0 \tag{25b}$$

$$\bar{H}(X = 1, \tau) = e^{-\gamma t} \tag{25c}$$

Where,

$$\gamma_1 = \frac{SL^2}{Kh\cos^2 \beta} \tau \tag{26}$$

Laplace transform techniques is used to find a solution; definition of the transform is as follows:

$$L\left\{ \bar{H}(X,\tau)\tau \to p \right\} = \theta(X,p) = \int_0^\infty e^{-p\tau} H\left(X,\tau\right) d\tau \tag{27}$$

Applying the transform to both sides of Eq. (23) and on solving the resulting ordinary differential equation with the standard method, we get

$$\begin{aligned}
\theta(X,p) = {} & \left(\frac{2\alpha - N_0{}'}{p^2} \right) \left\{ e^{\alpha X} \frac{\sinh\left\{ (1-X)\left(\sqrt{\alpha^2 + p} \right) \right\}}{\sinh\left(\sqrt{\alpha^2 + p} \right)} + e^{-\alpha(1-X)} \frac{\sinh\left(\sqrt{\alpha^2 + p} \right) X}{\sinh\left(\sqrt{\alpha^2 + p} \right)} - 1 \right\} \\
& + \frac{N_1{}'}{p\left(p + \lambda_1\right)} \left\{ -e^{\alpha X} \frac{\sinh\left\{ (1-X)\left(\sqrt{\alpha^2 + p} \right) \right\}}{\sinh\left(\sqrt{\alpha^2 + p} \right)} - e^{-\alpha(1-X)} \frac{\sinh\left(\sqrt{\alpha^2 + p} \right) X}{\sinh\left(\sqrt{\alpha^2 + p} \right)} + 1 \right\} \\
& + e^{-\alpha(1-X)} \left\{ \frac{1}{\left(p + \gamma_1\right)} \frac{\sinh\left(\sqrt{\alpha^2 + p} \right) X}{\sinh\left(\sqrt{\alpha^2 + p} \right)} \right\} - e^{-\alpha(1-X)} \left\{ \frac{1}{p} \frac{\sinh\left(\sqrt{\alpha^2 + p} \right) X}{\sinh\left(\sqrt{\alpha^2 + p} \right)} \right\} + \frac{X}{p}
\end{aligned} \tag{28}$$

Now taking Laplace Inverse Transform on Eq. (28) and simplifying it. We obtain

$$\begin{aligned}\bar{H}(X,\tau) = X &- \left(2\alpha - N_0'\right)\sum_{n=1}^{\infty}\frac{2n\pi\left\{1-(-1)^n e^{-\alpha}\right\}e^{\alpha X}\sin n\pi X}{\left(\alpha^2+n^2\pi^2\right)^2}\left\{1-e^{-\left(\alpha^2+n^2\pi^2\right)\tau}\right\} \\ &+ \frac{N_1'}{\lambda_1}\left(1-e^{-\lambda_1\tau}\right) - \frac{N_1'}{\lambda_1}\left(1-e^{-\lambda_1\tau}\right)e^{\alpha X}\left[\frac{\sinh\left\{(1-X)\sqrt{\alpha^2-\lambda_1}\right\}+e^{-\alpha}\sinh\left(X\sqrt{\alpha^2-\lambda_1}\right)}{\sinh\left(\sqrt{\alpha^2-\lambda_1}\right)}\right] \\ &+ N_1'\sum_{n=1}^{\infty}\frac{2n\pi\left\{1-(-1)^n e^{-\alpha}\right\}e^{\alpha X}\sin n\pi X}{\left(\alpha^2+n^2\pi^2\right)\left(\alpha^2+n^2\pi^2-\lambda_1\right)}\left\{1-e^{-\left(\alpha^2+n^2\pi^2\right)\tau}\right\} - e^{-\alpha(1-X)}\frac{\sinh(\alpha X)}{\sinh(\alpha)} \\ &+ e^{-\alpha(1-X)}\frac{\sinh\left(\sqrt{\alpha^2-\gamma_1}\right)X}{\sinh\left(\sqrt{\alpha^2-\gamma_1}\right)}e^{-\gamma_1\tau} - e^{-\alpha(1-X)}\sum_{n=1}^{\infty}\frac{2n\pi(-1)^n\sin n\pi X\, e^{-(\alpha^2+n^2\pi^2)\tau}}{\left(\alpha^2+n^2\pi^2\right)} \\ &+ e^{-\alpha(1-X)}\sum_{n=1}^{\infty}\frac{2n\pi(-1)^n\sin n\pi X}{\left(\alpha^2+n^2\pi^2-\gamma_1\right)}e^{-\left(\alpha^2+n^2\pi^2\right)\tau}\end{aligned} \quad (29)$$

Eq. (29) provides a closed-form analytical expression for the approximation of water head distribution in the aquifer.

4. Discussions of Results

Three separate FORTRAN codes are written to implement Mac Cormack scheme, DFF schemes, and approximate analytical solution as derived in preceding sections. Since the stability criterion of the numerical schemes are different, we have chosen $\Delta x = 1m, \Delta t = 0.001d$ for Mac Cormack scheme, and $\Delta x = 0.1m, \Delta t = 0.001d$ for DFF scheme. Values of other aquifer parameters are: K = 2.5 m/h, S = 0.2, L = 100 m, h_0 = 5 m, h_L = 3 m, N_0 = 4 mm/h, N_1 = 2 mm/h, λ = 0.2 day–1, γ = 0.2 day–1. Water table fluctuations for β = 3 deg, 0 deg, and – 5 deg are plotted in Figure 1 – Figure 3 using approximate analytical (represented by continuous curves) and numerical (represented by dotted curves) solutions. The observation that the dotted curves are "almost indistinguishable" suggests that the numerical and analytical solutions are quite close to each other, especially in the overall behavior. Water table variations in Figure 2, Figure 3, and Figure 4 are likely showing the changes in water table levels for different bed slopes, demonstrating how the water table responds to external conditions. Bed slope affects the hydraulic gradient, which in turn affects groundwater flow and the resulting water table configuration. As the slope increases, water may drain faster, impacting the water table height over time. The analytical solution underestimates the water table variation during the initial period of stream rise. This could be due to the fact that analytical methods often involve simplifications, such as assuming steady-state conditions, which may not capture the transient dynamics of the system, particularly in the early stages of the stream rise when changes are rapid. As time progresses, the discrepancy between the analytical and numerical solutions increases. This might occur because, in the real-world scenario (which the numerical solution approximates more closely), factors such as non-linearities, boundary effects, or other transient phenomena become more significant over time. Analytical solutions might fail to account for these complexities, leading to larger deviations from the actual scenario. Eventually, for large values of time, the difference between the analytical and numerical solutions diminishes. This suggests that both approaches converge to a steady-state or equilibrium solution. At this point, the system's dynamics slow down, and the simplifications made in the analytical model become more accurate, as transient effects are less important in the long term.

Dynamic profiles of the water table indicate the formation of groundwater mound in the middle part of the aquifer due to continuous downward percolation. Numerical experiments reveal that the height of the mound increases with time and eventually stabilizes after a large value of time (t = 120 hr). One more parameter- a bed slope is affecting the height of water head. As the downward bed sloping angle increases, water head in the middle part of the aquifer also grows higher primarily due to increase inflow from the left-hand water body. For an upward sloping aquifer (for instance β = – 5 deg), the mound height is significantly lower than that of a downward sloping aquifer.

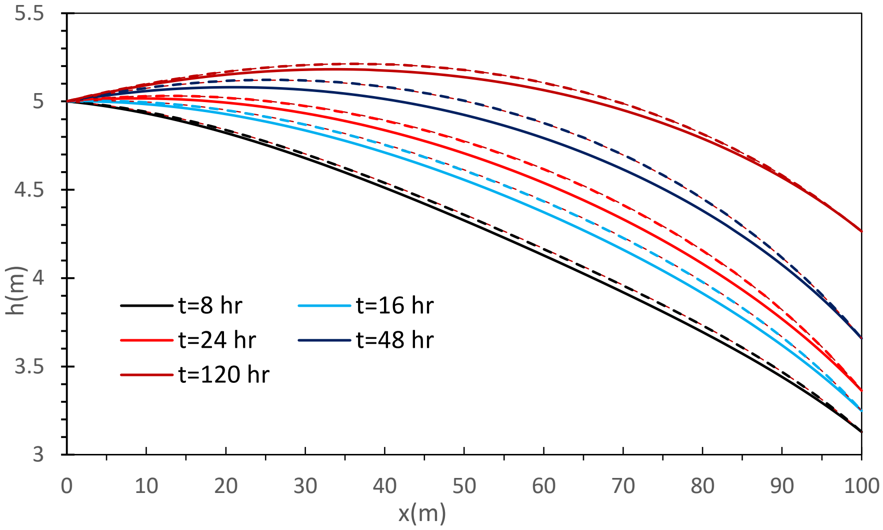

Fig. 2. Variation of water table height with 3 Deg sloping angle

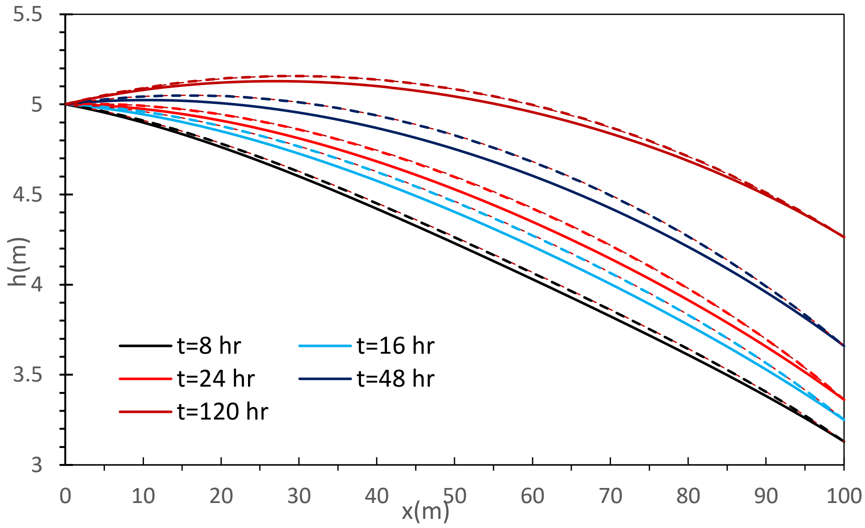

Fig. 3. Variation of water height for 0 Deg slope

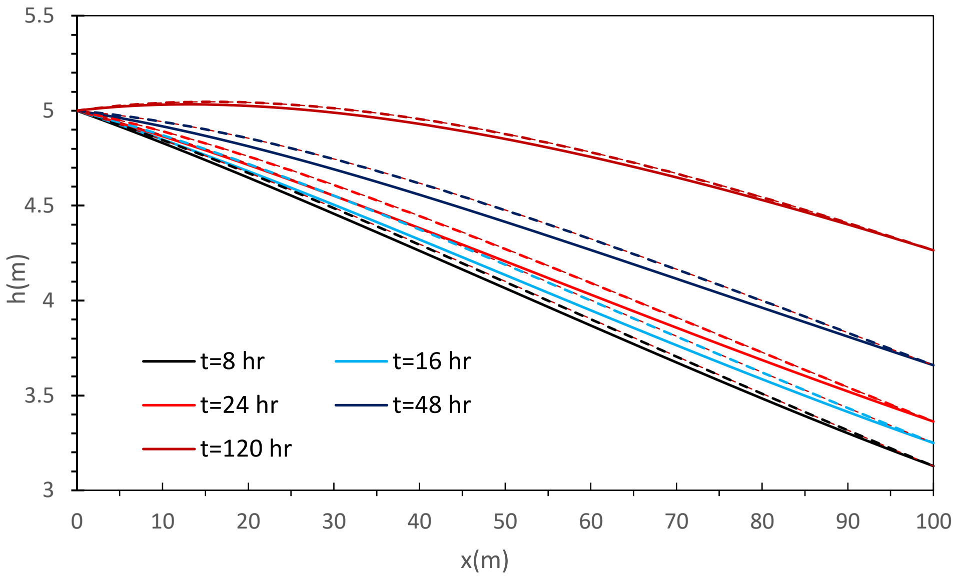

Fig. 4. Water table variation for downward -5 Deg slope

To Provide additional insight into this aspect, values of water head are calculated at x = 20, 40, 60, and 80 m using analytical and numerical solutions for β = 3, 0, and –5 deg. The same is presented in Table 1.

Table 1
Comparison of analytical (Ana) solution with Mac Cormack (MC) and DFF schemes

x	**t = 8 hrs**			**t = 16 hrs**			**t = 24 hrs**		
	Ana	MC	DFF	Ana	MC	DFF	Ana	MC	DFF
β = – 3 deg									
20	4.6958	4.7200	4.7180	4.7548	4.7905	4.7888	4.8004	4.8424	4.8409
40	4.3261	4.3606	4.3572	4.4257	4.4804	4.4775	4.5070	4.5720	4.5694
60	3.9319	3.9687	3.9653	4.0509	4.1101	4.1070	4.1544	4.2241	4.2215
80	3.5318	3.5613	3.5595	3.6551	3.6991	3.6979	3.7680	3.8190	3.8170
β = 0 deg									
20	4.7624	4.7829	4.7815	4.8504	4.8798	4.8788	4.9092	4.9447	4.9436
40	4.4202	4.4527	4.4498	4.5751	4.6263	4.6239	4.6821	4.7458	4.7429
60	4.0293	4.0674	4.0641	4.2114	4.2749	4.2716	4.3481	4.4247	4.4216
80	3.6093	3.6438	3.6421	3.7763	3.8322	3.8305	3.9140	3.9790	3.9774
β = 3 deg									
20	4.8213	4.8386	4.8375	4.9281	4.9514	4.9508	4.9925	5.0211	5.0208
40	4.5106	4.5405	4.5380	4.7105	4.7566	4.7543	4.8361	4.8937	4.8911
60	4.1278	4.1664	4.1632	4.3728	4.4376	4.4351	4.5382	4.6175	4.6153
80	**3.6935**	**3.7327**	**3.7308**	**3.9136**	**3.9795**	**3.9780**	**4.0798**	**4.1561**	**4.1548**

Numerical experiments were carried out to assess the variations between these solutions, and accordingly, a mathematical term namely Relative Percentage Difference (RPD) between numerical and analytical solutions is defined as follows:

$$RPD = \frac{\left|\hbar_{ana} - \hbar_{num}\right|}{\left|\hbar_{num}\right|} \times 100 \tag{30}$$

RPD is also useful in determining the validity range of the linearization process used in Eq. (22). Numerical experiments are carried out comprehensively by considering various values of aquifer parameters. Variation in RPD for β = 3 deg, 0 deg, and – 5 deg are plotted in Figure 5 to Figure 7 and its range for the same set of aquifer parameters is listed in Table 2. The general observations are as under:

i. RPD is least in the proximity of stream-aquifer interfaces and increases with spatial coordinate.
ii. Maximum value of RPD is observed in the middle part of the aquifer domain with a slight drift towards the x-axis.
iii. RPD increases with time. However, after attaining a maximum value, it eventually decreases. In our present case, it is maximum for t = 48 hr.
iv. Bed slope plays an important role in the variation of RPD. While for a downward sloping aquifer (β = 3 deg), the peak value of RPD is approximately 1.8 (for t = 24 hr); the same for an upward sloping aquifer (β = – 5 deg) is only 1.4.

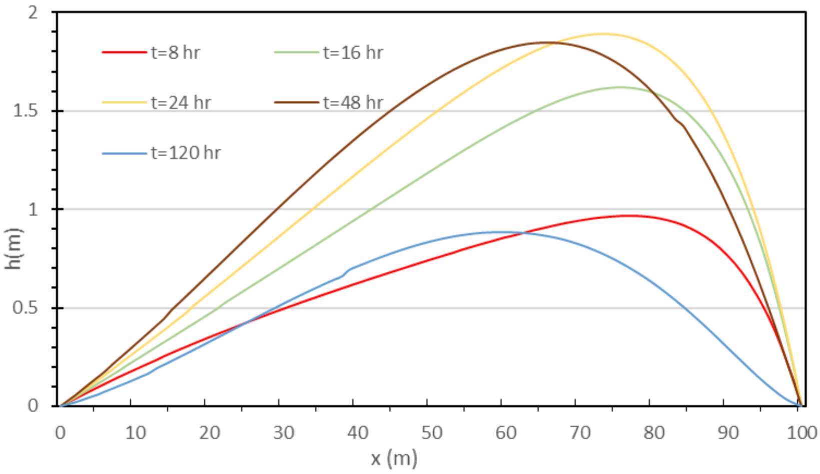

Fig. 5. Variation in RPD with x coordinate for various values of time t and β =3 deg

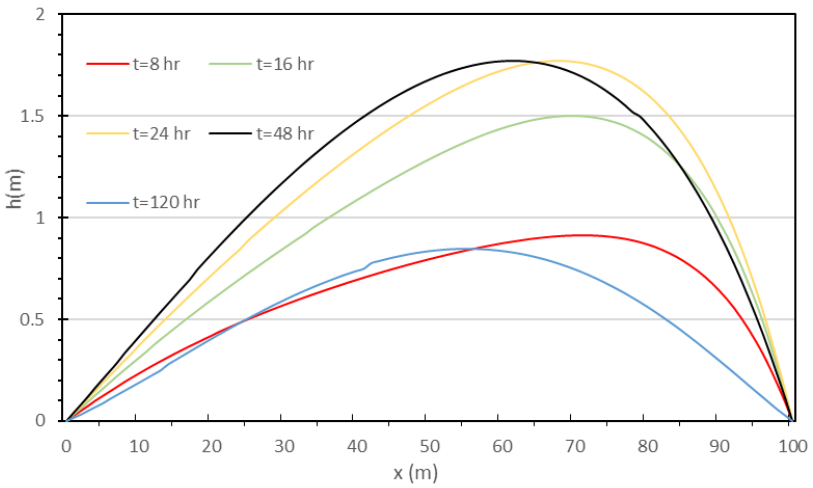

Fig. 6. Variation in RPD with x coordinate for various values of time t and β = 0 deg

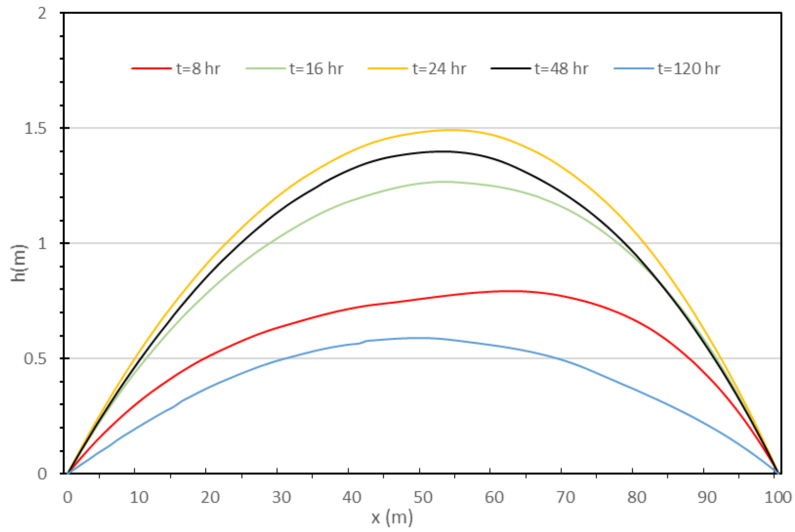

Fig. 7. Variation in RPD with x coordinate for various values of time t and β = –5 deg

Table 2
Range of RPD for various values of aquifer parameters

β	t = 8 hr	t = 16 hr	t = 48 hr
– 5	0.0 to 0.856650	0.0 to 1.332301	0.0 to 1.530806
– 3	0.0 to 0.873284	0.0 to 1.390075	0.0 to 1.628179
–1	0.0 to 0.873284	0.0 to 1.461102	0.0 to 1.725202
0	0.0 to 0.912161	0.0 to 1.499861	0.0 to 1.769619
1	0.0 to 0.928409	0.0 to 1.539857	0.0 to 1.813077
3	0.0 to 0.965016	0.0 to 1.617264	0.0 to 1.888561
5	0.0 to 1.009242	0.0 to 1.688382	0.0 to 1.945183

Another mathematical parameter used for assessing average distance between the analytical and numerical solutions is used here. This parameter, often referred to as L2 norm, is defined as follows:

$$\left(\frac{1}{\sqrt{L}}\right)\left\|\hbar_{num}-\hbar_{ana}\right\|=\left(\frac{1}{\sqrt{L}}\right)\left[\int_{x=0}^{L}\left\{\hbar_{num}(x,t)-\hbar_{ana}(x,t)\right\}\right]^{\frac{1}{2}} \tag{31}$$

Where the integral in the right-hand side calculated over the aquifer domain using Simpson's one-third rule. Numerical experiments for the same set of aquifer data is presented in Table 3. These data reveal that the distance between analytical and numerical solution is maximum in the middle part of the aquifer and negligible in proximity of X = 0 and X = 1. Furthermore, the T norm is smaller for upward sloping aquifers than that of downward sloping aquifers.

If suitability of solution determined by these norms, then the analysis presented in Table 2 and Table 3 demonstrate high rank of performance of analytical solutions developed in this study. Nevertheless, it is worth reiterating that linearization of advection-diffusion equation works well. The rank of performance of analytical solution in terms of the two norms broadly remains unaffected by variations in bed slopes.

Table 3
Range of L2 norm for various values of aquifer parameters

β	t = 8 hr	t = 16 hr	t = 48 hr
– 5	0.0 to 0.036288	0.0 to 0.057243	0.0 to 0.06631
– 3	0.0 to 0.036917	0.0 to 0.059495	0.0 to 0.070466
–1	0.0 to 0.037832	0.0 to 0.062447	0.0 to 0.074833
0	0.0 to 0.038453	0.0 to 0.064122	0.0 to 0.077014
1	0.0 to 0.039158	0.0 to 0.065880	0.0 to 0.079040
3	0.0 to 0.040769	0.0 to 0.069437	0.0 to 0.082879
5	0.0 to 0.042749	0.0 to 0.072936	0.0 to 0.086108

5. Conclusions

The work described in this study is focuses on analyzing a stream-aquifer model that considers subsurface seepage in a sloping unconfined aquifer under time-varying recharge. The main findings are as follows:

i. Model Development: The study involves the development of an approximate analytical solution and two numerical schemes to analyze the stream-aquifer model. This model considers the interaction between a stream or water body and an unconfined aquifer, considering factors such as subsurface seepage and time-varying recharge.
ii. Aquifer Recharge: The aquifer domain is recharged by both a nearby water body or stream with a constant water level and by time-varying water levels. This implies that the recharge into the aquifer varies over time, likely influenced by factors such as seasonal variations in precipitation or changes in stream flow.
iii. Dynamic Profiles: The study involves plotting dynamic profiles of the water table within the aquifer over time. These profiles provide insights into how the water table varies spatially and temporally within the aquifer domain under different sets of aquifer parameters and sloping angles.
iv. Comparison of Analytical and Numerical Solutions: The results obtained from the analytical solution are compared with those from the numerical solution to assess the validity of linearization. Linearization is a common simplification technique used in analytical solutions to make complex mathematical problems more tractable. The comparison likely involves evaluating how closely the analytical solution approximates the more computationally intensive numerical solution.
v. Observations: The study finds that the results from the analytical solution are in excellent agreement with those from the numerical solution for an upward-sloping aquifer. However, for downward-sloping beds, minor variations in the results are observed in the middle part of the aquifer domain. This suggests that the linearization assumptions may not perfectly capture the behavior of the system under certain conditions, particularly when the aquifer slopes downward.

Overall, the research contributes to understanding the dynamics of subsurface seepage in sloping unconfined aquifers under time-varying recharge conditions. It highlights the importance of considering factors such as aquifer slope and recharge variability in groundwater modeling and underscores the need for rigorous validation of modeling approaches through comparisons between analytical and numerical solutions.

Although, the experimental analysis is considered to be the most reliable technique for understanding the regional groundwater flow system; it has several limitations and disadvantages. Firstly, the experimental work in groundwater hydrology is an extremely costly affair. Moreover, it does not provide a holistic perspective in understanding the flow system and its dependence on various hydrologic parameters. On the other hand, the analytical approach is often the simplest and quickest way to obtain answers the questions posed by water-resource managers. Analytical models can also be instrumental in improving our understanding of physical processes occurring within a ground-water flow system. The model presented here provides a theoretical framework that can be adapted for groundwater management and serves as a foundation for future case studies or collaborations with water resource managers. The current study focused on specific bed slopes to ensure controlled analysis, future research could indeed expand the range of slopes to evaluate the model’s robustness under diverse conditions. This would allow for a more comprehensive understanding of its applicability in various real-world scenarios.

References

[1] Wooding, R. A., and T. G. Chapman. "Groundwater flow over a sloping impermeable layer: 1. Application of the Dupuit-Forchheimer assumption." *Journal of Geophysical Research* 71, no. 12 (1966): 2895-2902. https://doi.org/10.1029/JZ071i012p02903

[2] Childs, E. C. "Drainage of groundwater resting on a sloping bed." *Water Resources Research* 7, no. 5 (1971): 1256-1263. https://doi.org/10.1029/WR007i005p01256

[3] Hantush, Mahdi S. "Wells near streams with semipervious beds." *Journal of Geophysical Research* 70, no. 12 (1965): 2829-2838. https://doi.org/10.1029/JZ070i012p02829

[4] Saxena, Shikha, Rajeev Kumar Bansal, and Basant Kumar Singh. "Mathematical Modeling of Transient Water Interactions Between a Sloping Aquifer and an Adjusting Stream." *ECS Transactions* 107, no. 1 (2022): 11295.

[5] Marino, M. A. "Water-table fluctuation in semipervious stream-unconfined aquifer systems." *Journal of Hydrology* 19, no. 1 (1973): 43-52. https://doi.org/10.1016/0022-1694(73)90092-9

[6] Mohyud-Din, Syed T., Mustafa Inc, and Ebru Cavlak. "On numerical solutions of two-dimensional Boussinesq equations by using Adomian decomposition and He's homotopy perturbation method." *Applications and Applied Mathematics: An International Journal (AAM)* 5, no. 3 (2010): 1.

[7] Butler Jr, James J., Vitaly A. Zlotnik, and Ming-Shu Tsou. "Drawdown and stream depletion produced by pumping in the vicinity of a partially penetrating stream." (2001). https://doi.org/10.1111/j.1745-6584.2001.tb02354.x

[8] Serrano, Sergio E., and S. R. Workman. "Modeling transient stream/aquifer interaction with the non-linear Boussinesq equation and its analytical solution." *Journal of Hydrology* 206, no. 3-4 (1998): 245-255. https://doi.org/10.1016/S0022-1694(98)00111-5

[9] Parlange, J-Y., Francesco Stagnitti, A. Heilig, Jozsef Szilagyi, M. B. Parlange, T. S. Steenhuis, W. L. Hogarth, D. Andrew Barry, and L. Li. "Sudden drawdown and drainage of a horizontal aquifer." *Water resources research* 37, no. 8 (2001): 2097-2101. https://doi.org/10.1029/2000WR000189

[10] Verhoest, Niko EC, Valentijn RN Pauwels, Peter A. Troch, and François P. De Troch. "Analytical solution for transient water table heights and outflows from inclined ditch-drained terrains." *Journal of irrigation and drainage engineering* 128, no. 6 (2002): 358-364. https://doi.org/10.1061/(ASCE)0733-9437(2002)128:6(358)

[11] Verhoest, Niko EC, and Peter A. Troch. "Some analytical solutions of the linearized Boussinesq equation with recharge for a sloping aquifer." *Water Resources Research* 36, no. 3 (2000): 793-800. https://doi.org/10.1029/1999WR900317

[12] Pathania, Tinesh, Andrea Bottacin-Busolin, A. K. Rastogi, and T. I. Eldho. "Simulation of groundwater flow in an unconfined sloping aquifer using the element-free Galerkin method." *Water Resources Management* 33 (2019): 2827-2845. https://doi.org/10.4172/2157-7617.1000115

[13] Koussis, Antonis D., and Li-Ta Lien. "Linear theory of subsurface storm flow." *Water Resources Research* 18, no. 6 (1982): 1738-1740. https://doi.org/10.1029/WR018i006p01738

[14] Teloglou, Ilias S., and Rajeev K. Bansal. "Transient solution for stream–unconfined aquifer interaction due to time varying stream head and in the presence of leakage." *Journal of hydrology* 428 (2012): 68-79. https://doi.org/10.1016/j.jhydrol.2012.01.024

[15] Teloglou, E. S., and T. S. Zissis. "Unsteady drainage over semi-confined aquifer due to time-varying replenishment and drainage base." *Physics and Chemistry of the Earth, Part B: Hydrology, Oceans and Atmosphere* 24, no. 1-2 (1999): 145-150. https://doi.org/10.4172/2157-7617.1000115

[16] Rai, S. N., and A. Manglik. "An analytical solution of Boussinesq equation to predict water table fluctuations due to time varying recharge and withdrawal from multiple basins, wells and leakage sites." *Water resources management* 26 (2012): 243-252. https://doi.org/10.1007/s11269-011-9915-x
[17] Kalaidzidou-Paikou, N., D. Karamouzis, and D. Moraitis. "A finite element model for the unsteady groundwater flow over sloping beds." *Water resources management* 11 (1997): 69-81. https://doi.org/10.1023/A:1007926507718
[18] Sun, Jianping, Jiachun Li, Qingquan Liu, and Huiqin Zhang. "Approximate engineering solution for predicting groundwater table variation during reservoir drawdown on the basis of the Boussinesq equation." *Journal of Hydrologic Engineering* 16, no. 10 (2011): 791-797. https://doi.org/10.1061/(ASCE)HE.1943-5584.0000372
[19] Atangana, Abdon, and J. F. Botha. "Analytical solution of the groundwater flow equation obtained via homotopy decomposition method." *Journal of Earth Science & Climatic Change* 3, no. 2 (2012): 115. https://doi.org/10.4172/2157-7617.1000115
[20] Bansal, Rajeev K., and Samir Kumar Das. "Response of an unconfined sloping aquifer to constant recharge and seepage from the stream of varying water level." *Water resources management* 25 (2011): 893-911. https://doi.org/10.1007/s11269-010-9732-7
[21] Bansal, Rajeev K. "Groundwater fluctuations in sloping aquifers induced by time-varying replenishment and seepage from a uniformly rising stream." *Transport in porous media* 94 (2012): 817-836. https://doi.org/10.1007/s11242-012-0026-9
[22] Bansal, Rajeev K. "Approximate analytical solution of Boussinesq equation in homogeneous medium with leaky base." *Applications and Applied Mathematics: An International Journal (AAM)* 11, no. 1 (2016): 11.
[23] Lockington, D. A. "Response of unconfined aquifer to sudden change in boundary head." *Journal of Irrigation and Drainage Engineering* 123, no. 1 (1997): 24-27. https://doi.org/10.1061/(ASCE)0733-9437(1997)123:1(24)
[24] Parlange, J-Y., Francesco Stagnitti, A. Heilig, Jozsef Szilagyi, M. B. Parlange, T. S. Steenhuis, W. L. Hogarth, D. Andrew Barry, and L. Li. "Sudden drawdown and drainage of a horizontal aquifer." *Water resources research* 37, no. 8 (2001): 2097-2101. https://doi.org/10.1029/2000WR000189
[25] Hunt, Bruce. "Unsteady stream depletion from ground water pumping." *Groundwater* 37, no. 1 (1999): 98-102. https://doi.org/10.1111/j.1745-6584.1999.tb00962
[26] Lande, Chhaya K., Rajeev K. Bansal, and Arundhati Warke. "Simulation of two dimensional subsurface seepage flow in isolated anisotropic aquifer." *Materials Today: Proceedings* 23 (2020): 329-337. https://doi.org/10.1016/j.matpr.2020.02.032
[27] Huang, Ching-Sheng, Shaw-Yang Yang, and Hund-Der Yeh. "Groundwater flow to a pumping well in a sloping fault zone unconfined aquifer." *Water Resources Research* 50, no. 5 (2014): 4079-4094. https://doi.org/10.1002/2013WR014212
[28] Hsieh, Ping-Cheng, Jing-Lun Huang, and Ming-Chang Wu. "Response of groundwater levels in a coastal aquifer to tidal waves and rainfall recharge." *Water* 12, no. 3 (2020): 625. https://doi.org/10.3390/w12030625
[29] Shaikh, Bushra Y., Rajeev K. Bansal, and Samir K. Das. "Propagation of tidal wave in coastal terrains with complex bed geometry." *Environmental Processes* 5 (2018): 519-537. https://doi.org/10.1007/s40710-018-0314-7
[30] Mahdavi, Ali, Ying-Fan Lin, and Hwa-Lung Yu. "Well hydraulics in wedge-shaped aquifer: Unsteady Darcian flow model revisited by lagging theory." *Journal of Hydrology* 615 (2022): 128672. https://doi.org/10.1016/j.jhydrol.2022.128672
[31] Banerjee, Dolon, and Sayantan Ganguly. "A review on the research advances in groundwater–surface water interaction with an overview of the phenomenon." *Water* 15, no. 8 (2023): 1552. https://doi.org/10.3390/w15081552
[32] Lande, Chhaya, Shilpa Malge, B. S. Veena, and Ketan Kotecha. "Mathematical Modeling of Groundwater Surface Water Interaction Represented using Boussinesq Equation–A Bibliometric Study." *Journal of Advanced Research in Fluid Mechanics and Thermal Sciences* 111, no. 1 (2023): 96-108. https://doi.org/10.37934/arfmts.111.1.96108
[33] Becke, A. L., S. C. Solórzano-Rivas, and A. D. Werner. "The watertable fluctuation method of recharge estimation: A review." *Advances in Water Resources* (2024): 104635. https://doi.org/10.1016/j.advwatres.2024.104635
[34] Jaiswal, Dilip K. "Study of specially and temporally dependent adsorption coefficient in heterogeneous porous medium." *Applications and Applied Mathematics: An International Journal (AAM)* 14, no. 1 (2019): 34.
[35] Beleyur, Veena Sreenivasa. "Exploring the Dynamic Behavior of a Tapered Stenosed Artery: An Investigation into Its Unsteady Model." *Journal of Advanced Research in Fluid Mechanics and Thermal Sciences* 121, no. 2 (2024): 48-64. https://doi.org/10.37934/arfmts.121.2.4864